Investigation of Microphase Separation and Thermal Properties of Noncrystalline Ethylene Ionomers. 2. IR, DSC, and Dielectric Characterization

Shoichi Kutsumizu,*,† Kenji Tadano,‡ Yuki Matsuda,§ Masahiro Goto,§ Hitoshi Tachino,⊥ Hisaaki Hara,⊥,& Eisaku Hirasawa,⊥,^ Hiroyuki Tagawa,# Yoshio Muroga,$ and Shinichi Yano§

Instrumental Analysis Center, Gifu University, 1-1 Yanagido, Gifu 501-1193, Japan; Gifu College of Medical Technology, Ichihiraga, Seki, Gifu 501-3892, Japan; Department of Chemistry, Faculty of Engineering, Gifu University, 1-1 Yanagido, Gifu 501-1193, Japan; Technical Center, Du Pont-Mitsui Polychemicals Co., Ltd., 6 Chigusa-kaigan, Ichihara, Chiba 299-0108, Japan; Department of Applied Chemistry, Nihon University Junior College, 1-8-14 Kanda-Surugadai, Chiyoda-ku, Tokyo 101-0062, Japan; and School of Engineering, Nagoya University, Furo-cho, Chikusa-ku, Nagoya 464-8603, Japan

Received March 8, 2000

ABSTRACT: The microphase structure of noncrystalline poly(ethylene-*co*-13.3 mol % methacrylic acid) (E-0.133MAA) ionomers was investigated by using infrared (IR) spectroscopic, X-ray scattering, differential scanning calorimetric (DSC), and dielectric measurements. The noncrystallinity was confirmed by small-angle X-ray scattering (SAXS) and DSC studies, which has enabled a quantitative analysis of the SAXS ionic peak associated with ionic aggregates without being perturbed by the polyethylene lamellae peak. In 60% neutralized Na ionomer, it was revealed that almost 100% of MAA side groups including unneutralized COOH are incorporated into the ionic aggregates with an average ionic core radius (R_1) of ∼6 Å. The dielectric relaxation studies showed that the ionic aggregates form a microphase-separated ionic cluster. Analysis of dielectric strengths indicated the most (∼90%) of the COONa groups are present in the ionic cluster. On the other hand, in the 60% neutralized Zn ionomer, both SAXS and dielectric studies indicated that the ionic aggregates with $R_1 \sim 4$ Å are almost isolated and dispersed in the matrix; the formation of ionic cluster was not recognized. Similarly to partly crystalline E-MAA ionomers, all noncrystalline E-0.133MAA ionomers exhibited an endothermic peak at 320−330 K (labeled T_i) on the first heating, depending on the aging time at room temperature. Several factors that would be critical for the DSC T_i peak were discussed. It was concluded that the DSC T_i peak is certainly associated with changes of the state of ionic aggregate region.

Introduction

In 1964, Rees et al.[1,2] first developed poly(ethylene-*co*-methacrylic acid) (E-MAA) ionomers and opened the first page of ionomer industries. Ever since, various types of ionomers have been synthesized, and an enormous number of studies have been devoted to understand the structure−morphology−property relationships of these ionomers. It is now generally accepted that ionomers owe their peculiar properties to the aggregation of ionic groups introduced to the polymer backbone.[3−7] In partly crystalline ionomers such as E-MAA ionomers, the crystallinity also gives a profound influence on the ionic aggregation.[8−14] To avoid such complexity, much more fundamental studies have been focused on noncrystalline ionomers such as *atactic* polystyrene ionomers, which is now the best understood family among ionomers.[15,16] From an industrial point of view, however, E-MAA ionomers are still very important and widely used as excellent thermoplastics in use for packaging, extrusion coating, and molding applications.[17,18] To control the performance, more complete understanding of the structure−morphology−property relationships is demanded, but unfortunately, the present morphological picture has not been improved so much from Longworth's classical and qualitative three-phase model, which was proposed more than 30 years ago.[19] Therefore, it must be said that qualitative information on E-MAA ionomers is still very poor regarding the size of ionic aggregate and the number of ionic groups per aggregate.

Another important but unsolved problem on E-MAA ionomers is the presence of an anomaly observed at around 330 K below the melting point ($T_m \sim 360$ K) of polyethylene crystalline regions; the sample exhibits only a DSC T_m peak on heating immediately after cooling from the melt, but when stored at room temperature for more than several days, another endothermic peak appears at around 330 K below T_m. This peak was first found by Marx and Cooper, who ascribed it simply to the melting of imperfect crystallites of polyethylene short segments.[9] Very recently, this explanation was replaced by the same research group with a new interpretation that the endotherm is due to some change associated with the release of absorbed water from the ionic aggregate regions.[20] Earlier than Cooper's first report, MacKnight and co-workers proposed the

† Instrumental Analysis Center, Gifu University.
‡ Gifu College of Medical Technology.
§ Faculty of Engineering, Gifu University.
⊥ Du Pont-Mitsui Polychemicals Co.
Nihon University Junior College.
$ Nagoya University.
& Current address: Chiba Fac., Du Pont-Mitsui Polychemicals Co., Ltd., 6 Chigusa-kaigan, Ichihara, Chiba 209-0108, Japan.
^ Current address: Research Labo., Fujimori Kogyo Co., Ltd., No. 56 Imaikami-cho, Nakahara-ku, Kawasaki, Kanagawa 211-0067, Japan.
* To whom correspondence should be addressed. E-mail: kutsu@cc.gifu-u.ac.jp.

10.1021/ma0004256 CCC: $19.00
Published on Web 11/03/2000

existence of a glass−rubber transition of ionic aggregate regions around 330 K on the basis of their mechanical studies and so on,[21−24] but their papers did not refer to the DSC endotherm in this temperature region. In 1987, Tadano et al. proposed an order−disorder transition model of ionic aggregate regions:[25−27] Room-temperature aging of the sample causes some ordered structure inside the ionic aggregate regions, which is transformed into a disordered state at around 330 K on heating. The model was primarily based on the DSC and dilatometric data, but other various measurements by this research group also support the model.[12,28−37] Briefly speaking, thus, there have been four models treating the anomaly around 330 K, but no definitive evidence can support one of these models because of the colloidal size of the ionic aggregate region. On the other hand, Hirasawa et al. pointed out that the enthalpy change of this "transition" around 330 K and its growth with room-temperature aging closely correlate with some physical properties such as yield strength, surface hardness, and bending modulus and their change with the aging time, respectively.[12] Therefore, understanding the origin of this anomaly is important not only from an academic point of view but also from an industrial viewpoint, and this is a reason our research group has been adhering to this problem for a decade.

As mentioned above, the physical and thermal properties of E-MAA ionomers are profoundly influenced by the existence of polyethylene crystalline regions as well as ionic aggregate regions. MacKnight et al. pointed out that the crystallinity decreases almost linearly with the increase of methacrylic acid (MAA) content,[10] and in fact, E-MAA with a high content of MAA such as 20.4 mol % was reported to be noncrystalline.[38] Such noncrystalline E-MAA ionomers are useful to clarify the contribution of crystallinity to both the microphase-separation structure and the anomaly around 330 K in E-MAA ionomers. We chose in this study E-MAA ionomers containing 13.3 mol % of MAA, because this content of MAA was found to be a minimum content to make E-MAA copolymers noncrystalline, as will be shown in Figure 6 of this paper, and such a minimum content also would ensure the continuity of the physical properties to those of commercially important crystalline E-MAA ionomers with lower MAA contents. Hereafter, the E-MAA ionomers containing 13.3 mol % of MAA are denoted as E-0.133MAA-*x*M, where M indicates the type of metal cation and *x* is the degree of neutralization.

In this paper, the microphase structure and thermal properties of noncrystalline E-0.133MAA ionomers were investigated by use of IR spectroscopic, X-ray scattering, DSC, and dielectric measurements. One of the purposes of this paper is to obtain quantitative information on the structure as much as possible, and a combination of several measurement techniques would make the interpretation unambiguous and enable to justify the evaluation. Since our continuing target is partly crystalline E-MAA ionomers, the results are compared with those of partly crystalline E-MAA ionomers and discussed.

Experimental Section

Materials. The precursor E-0.133MAA was from Du Pont-Mitsui Polychemicals Co. Ltd., whose melt index is 930 g/10 min; the melt index was measured as the weight of polymer flow (g/10 min) from a melt indexer at 463 K and under a 2160 g load. The metal salts of E-0.133MAA were prepared by a melt reaction of E-0.133MAA with a stoichiometric amount of Na_2CO_3 or ZnO using a Toyoseiki Laboplastomill at 493 K for 15 min. At the end of 15 min, the samples were immediately removed and compression-molded into sheets with a suitable thickness (0.03−0.5 mm) at 15 MPa and at 453 K and then cooled to room temperature at a cooling rate of 30 K/min. The sheets obtained in this way were transparent and showed no signs of unreacted metal salts, which was also checked by IR, SAXS, and WAXS, indicating that the reaction proceeded stoichiometrically. To avoid moisture absorption, all samples were stored in a vacuum desiccator prior to use but were found to contain a trace of water. The amounts of water contained, determined from the weight loss by vacuum-drying at 423−453 K for 1 h,[31] were 1.33 wt % [$0.2H_2O$/COOH] for E-0.133MAA, 0.46 wt % [$0.3H_2O/Na^+$] for E-0.133MAA-0.2Na, 0.81 wt % [$0.2H_2O/Na^+$] for E-0.133MAA-0.6Na, and 0.26 wt % [$0.2H_2O/Zn^{2+}$] for E-0.133MAA-0.6Zn. These amounts are not so much compared to the case of dry E-0.054MAA ionomers (0.22 wt % [$0.07H_2O$/COOH] for E-0.054MAA, 0.24 wt % [$0.4H_2O/Na^+$] for E-0.054MAA-0.2Na, 0.29 wt % [$0.2H_2O/Na^+$] for E-0.054MAA-0.6Na, and 0.084 wt % [$0.2H_2O/Zn^{2+}$] for E-0.054MAA-0.6Zn).[32] To avoid such small absorption of water during the storage of the samples, more rigorous conditions are needed, which is often unable to be employed, and so, most of the experiments were made for these "dry" samples. In separate experiments, the effect of such a small amount of water on the DSC behavior was also checked by using completely dried samples with great care for water absorption (see the section T_i and Water Absorption).

Other E-MAA samples examined for comparison were also from Du Pont-Mitsui, and their ionomers were prepared by the same neutralization technique mentioned above.[12]

Measurements. Infrared (IR) spectra were measured with a Perkin-Elmer 1640 FTIR spectrometer at room temperature, where 32 or 64 scans at a resolution of 4 cm^{-1} were signal averaged.

Small-angle X-ray scattering (SAXS) experiments were carried out at the Photon Factory beamline 10C, the National Laboratory for High Energy Physics, Tsukuba, Japan. The synchrotron radiation monochromatized (λ = 1.488 Å) and a point-focusing optics were used. The scattered profiles were recorded by a linear position-sensitive proportional counter (PSPC) and corrected for parasitic scattering (background scattering), sample absorption, and beam intensity decay and were normalized to 1 mm sample thickness. The details of the optics and data treatments are described elsewhere.[39,40]

Wide-angle X-ray scattering (WAXS) measurements were performed with a Mac Science X-ray diffractometer (MXP^3 system) in the Instrumental Center, Institute of Molecular Science, Okazaki, Japan. The measurement conditions were the same as described elsewhere.[31]

Differential scanning calorimetric (DSC) thermograms were recorded by using a Seiko Denshi DSC-210 (SSC-5000 system), which was calibrated by indium (mp 156.6 °C, ΔH = 28.458 cal g^{-1}) and tin (mp 231.9 °C, ΔH = 59.5 cal g^{-1}). The measurements were done under a dry N_2 flow of ca. 40 mL/min, and the scanning rates used were 5 and 10 K min^{-1}. About 10 mg of the sample aged at room temperature for more than 30 days was weighed to 10^{-2} mg, packed into an aluminum pan, and used. In the first heating from room temperature, partly crystalline E-MAA ionomers show two endothermic peaks at ∼330 and ∼360 K, and the former is the anomaly mentioned in the Introduction and the latter is the T_m peak. The weight fraction of polyethylene crystallinity (X_c) was calculated from the enthalpy change at T_m by assuming that the heat of fusion of polyethylene crystallites is 290.4 J/g.

Thermal expansions were measured at a heating/cooling rate of ca. 0.5 K/min using a glassy capillary dilatometer (0.6 mm i.d.). A compression-molded sheet of ∼1 g was aged at room temperature for more than 30 days and then carefully immersed in liquid mercury in vacuo to avoid the formation of voids on the surface of the sheet. The volume change was calculated from a reading of the height of mercury in the capillary of the dilatometer. The density at 298 K was obtained by a buoyancy method with acetonitrile.

Dielectric measurements were carried out with an LCR meter (Yokogawa-Hewlett-Packard, type 4274A) attached to an NEC PC9801F2 computer, by use of the three-terminal electrode system described previously.[41] The specimens were circular sheets of ca. 0.5 mm thickness. To ensure electrical contact between the electrode and the specimen, gold was carefully deposited in vacuo on the surface of the specimen, and then, the specimen was aged at room temperature for 30−50 days. The measurements were made under dry N_2 gas atmosphere. The temperature was monitored by a calibrated Fe−constantan thermocouple.

Results and Discussion

IR Spectra. Noncrystalline E-0.133MAA ionomers prepared in this work were first studied by IR spectroscopy. Neutralization of E-0.133MAA with Na or Zn decreases the intensity of the carbonyl stretching [ν(C═O)] vibrational band at 1698 cm^{-1} and produces new bands attributable to carboxylate asymmetric stretching [$\nu_{as}(COO^-)$] vibrations in the region 1500−1650 cm^{-1}.[42] In E-0.133MAA-0.6Na, the $\nu_{as}(COO^-)$ band is very broad, and its maximum is located at 1555 cm^{-1}. The envelope of this band is similar to that observed in the Na salts with lower MAA contents, indicating that the coordination structure around Na cation is the same in both E-0.133MAA-0.6Na and the Na salts with lower MAA contents. On the other hand, E-0.133MAA-0.6Zn exhibits two sharp peaks at 1539 and 1624 cm^{-1} with a weak shoulder peak at 1584 cm^{-1} in the $\nu_{as}(COO^-)$ band region. This result is in contrast with the $\nu_{as}(COO^-)$ band of the Zn(II) salts with lower MAA such as E-0.054MAA-0.6Zn, because in the latter Zn(II) salts a strong peak is observed at 1585 cm^{-1} with two weak shoulder peaks at 1539 and 1624 cm^{-1}.

According to Coleman et al.,[43] the band at 1585 cm^{-1} is assigned to a tetracoordination structure around Zn(II), and this assignment is also supported by extended X-ray absorption fine structure (EXAFS) studies.[30,44,45] The assignment of the 1539 and 1624 cm^{-1} bands is, on the other hand, still a subject to debate. Coleman et al.[43] assigned these two bands to an acid salt structure whose coordination number around Zn(II) is apparently larger than 4. Ishioka[46,47] and Grady and co-workers[48] assigned them to a tetracoordination structure of Zn(II) where some of oxygen atoms of carboxylate groups are replaced by those of water molecules because of water absorption of the sample. Very recently, we found that the $\nu_{as}(COO^-)$ bands of E-0.054MAA-0.6Zn show a spectral change from the 1539 and 1624 cm^{-1} bands to the 1584 cm^{-1} band when the pressure applied to the sample at 400 K in the melt is increased from 0 (vacuum) to 4 MPa.[49] Since this change was observed at 400 K in the melt, the transformation of the coordination structure around Zn(II) does not necessarily need water absorption, and therefore, the assignment by Coleman et al. is more plausible. Although it is more realistic to consider that various types of coordination structures are present in the sample from tetra- to hexacoordination structures, including the Coleman's type, the hexacoordination structure is regarded as an ultimate structure, and in this meaning, we simply assigned the 1539 and 1624 cm^{-1} bands to the hexacoordination structure around Zn(II). Thus, it is concluded that most of the Zn(II) cations in E-0.133MAA-0.6Zn form the hexacoordination structure, and the content of MAA affects the coordination structure around Zn(II).

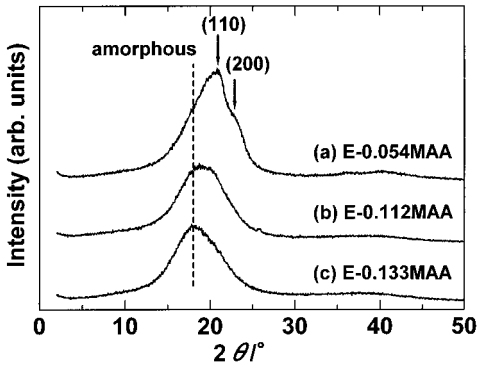

Figure 1. WAXS patterns at room temperature of (a) E-0.054MAA, (b) E-0.112MAA, and (c) E-0.133MAA. (110) and (200) indicate the reflections from orthorhombic polyethylene crystallites.

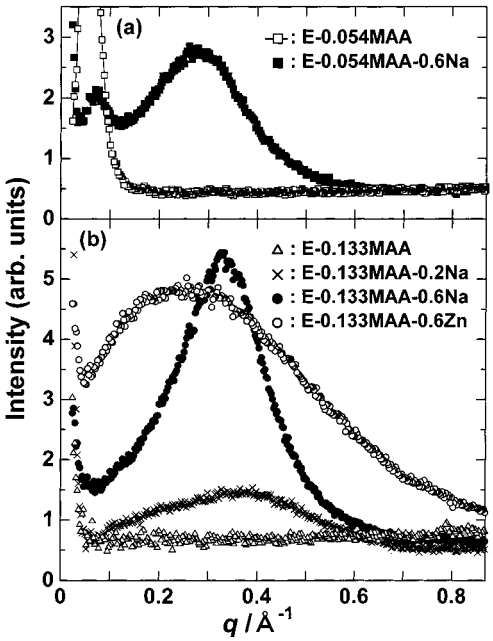

Figure 2. SAXS patterns at room temperature of (a) E-0.054MAA and (b) E-0.133MAA ionomers: E-0.054MAA (□), E-0.054MAA-0.6Na (■), E-0.133MAA (△), E-0.133MAA-0.2Na (×), E-0.133MAA-0.6Na (●), and E-0.133MAA-0.6Zn (○).

X-ray Scattering. Figure 1 shows WAXS patterns for three ionomer precursors containing various MAA contents: E-0.054MAA, E-0.112MAA, and E-0.133MAA. Partly crystalline E-0.054MAA in (a) shows a peak at 20.9° and a shoulder peak at 23.2°, which are assigned respectively to (110) and (200) diffraction peaks of polyethylene crystallites of orthorhombic type.[19,50] A shoulder peak around 18°, although not evident in (a), comes from the amorphous polyethylene regions. In E-0.112MAA in (b), the (110) and (200) diffraction peaks are mostly depressed, and in E-0.133MAA in (c) only the amorphous peak is seen centered at 18.0°. These observations are consistent with the degree of polyethylene crystallinity estimated from the DSC data (see below).

Figure 2 shows the SAXS patterns for (a) partly crystalline E-0.054MAA ionomers and (b) noncrystalline E-0.133MAA ionomers. In (a), E-0.054MAA-0.6Na ionomer exhibits two peaks at $q = 0.07$ and 0.27 $Å^{-1}$, where $q = (4\pi/\lambda) \sin\theta$, and λ and 2θ are the wavelength and scattering angle of X-ray, respectively. The broad peak at $q = 0.27$ $Å^{-1}$, absent in the acid form E-0.054MAA,

Table 1. Model Fit Parameters for Noncrystalline E-0.133MAA and Partly Crystalline E-0.054MAA Ionomers[a]

sample	R_1/Å	R_{ca}/Å	n(MAA)	β	r_{max} (/Å) of $p(r)$
E-0.133MAA-0.2Na	4.8	6.7	6	0.6	4.7, 17 (weak)
E-0.133MAA-0.6Na	5.7	7.9	9	1.0	5.2, 22, 41
E-0.133MAA-0.6Zn	4.1	6.9	3	0.09	4.1
E-0.054MAA-0.6Na	6.3	8.7	12.5	1.0	−

[a] R_1, radius of ionic core of ionic aggregate; R_{ca}, radius of outer hydrocarbon shell of ionic aggregate; n(MAA), average number of MAA side groups (both neutralized and unneutralized) that are in an aggregate; β, fraction of the side groups incorporated into aggregates; $p(r)$, distance distribution function; r_{max}, the r value at which $p(r)$, that is, the distribution of interaggregate distance, shows a maximum; −, unable to calculate because of its crystallinity.

is due to the formation of ionic aggregates in this ionomer[19,50−52] and often called an *ionic peak*. On the other hand, the peak at $q = 0.07$ Å^{-1}, which is also seen in E-0.054MAA, is ascribed to the presence of polyethylene lamellae in the sample.[14,52] In (b), E-0.133MAA ionomers and their acid precursor exhibit no polyethylene peak in the region $q = 0.02-0.10$ Å^{-1}, which reflects their noncrystallinity. For three E-0.133MAA ionomers, the ionic peak is seen at 0.37 Å^{-1} for E-0.133MAA-0.2Na, at 0.33 Å^{-1} for E-0.133MAA-0.6Na, and at 0.26 Å^{-1} for E-0.133MAA-0.6Zn. The peak of E-0.133MAA-0.6Zn is very broad whereas that of E-0.133MAA-0.6Na is comparatively sharp, indicating the difference in the formation of ionic aggregates between the two metal cations. The characteristic parameters based on the Yarusso and Cooper's liquid-like model[51,52] are summarized in Table 1. The full discussion on the validity of this model is reported separately,[40] and here the important conclusions useful for the discussion on the microphase structure in connection with the dielectric results later mentioned are given.

In Table 1, comparison between E-0.133MAA-0.6Na and -0.6Zn gives the following picture: In the Na salt, the ionic aggregate has a large chance of being neighbored by other aggregates, as shown by three well-defined maxima on the distance distribution function $p(r)$, whereas in the Zn(II) salt, the $p(r)$ shows only one well-defined peak at ∼4.7 Å, indicating that the ionic aggregate is almost isolated and dispersed in the matrix. It should be here mentioned that noncrystallinity of E-0.133MAA ionomers is a key factor for obtaining the above conclusions, and in partly crystalline E-MAA ionomers the neighboring polyethylene peak makes difficult such a full analysis of ionic peak without ambiguity.

DSC and Dilatometry. Figure 3 shows the DSC and specific volume ($V(T)$)−temperature (T) curves for E-0.133MAA and E-0.133MAA-0.6Na on the first heating, where both samples were aged at room temperature for more than 1 month after compression-molding at 453 K. Table 2 summarizes the DSC parameters, which includes the data of E-0.133MAA-0.2Na and E-0.133MAA-0.6Zn. For the acid E-0.133MAA, the DSC curve (in (c)) shows a step at around 286 K and an endothermic peak at 322 K, and correspondingly, on the $V(T)-T$ curve (in (a)), a well-defined bend is seen at 283 K and a step is seen at 315 K. Here, the step temperature was determined from a peak temperature on the first derivative of the $V(T)-T$ curve. Clearly, the anomaly near 285 K is assigned to the glass transition (T_g) of the backbone, and the noncrystallinity enables the detection. Coleman et al.[38] reported that E-0.204MAA

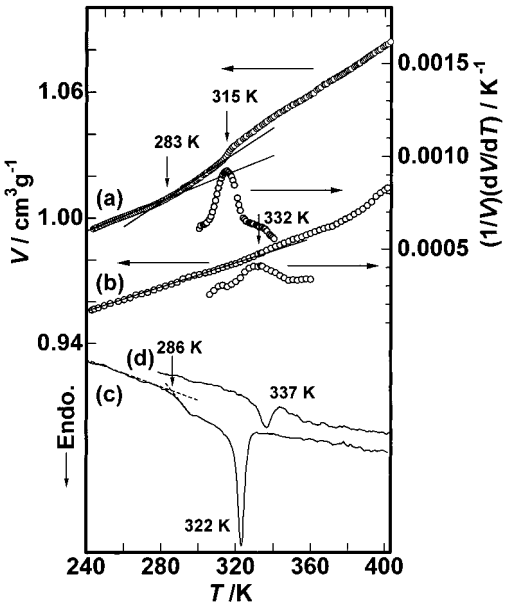

Figure 3. Specific volume (V) versus temperature (T) curves and DSC curves of E-0.133MAA (a and c, respectively) and E-0.133MAA-0.6Na (b and d, respectively) on heating after aging at room temperature for more than 1 month. Solid and broken curves are only guides for the eye. In (a) and (b), thermal expansion coefficient [$(1/V)(dV/dT)$] versus T curves, referred to the right scale, are also shown in the range 300−350 K, which determine the temperature of T_i (see text).

Table 2. Specific Volume (V) at 298 K and DSC Parameters of E-0.133MAA Ionomers[a]

sample	V, cm^3/g	T_i, K	ΔH_i, J/g
E-0.133MAA	1.0178	322	9.9
E-0.133MAA-0.2Na	1.0017	322	4.2
E-0.133MAA-0.6Na	0.9727	343	3.3
E-0.133MAA-0.6Zn	0.9515	334	2.5

[a] V, specific volume at 298 K; T_i, order−disorder transition temperature of ionic aggregates; ΔH_i, enthalpy change at T_i.

and E-0.285MAA are noncrystalline and their T_g's are in the range 298−305 K, which are higher than the T_g of E-0.133MAA. This is clearly due to the higher contents of MAA, which increases the average rigidity of the backbone, in the former two polymers. On the other hand, our DSC studies revealed that E-0.112MAA, whose MAA content is slightly smaller than that of E-0.133MAA, is still crystalline, and the weight crystallinity is estimated at about 7% (see Figure 6). Therefore, it may be said that 13.3 mol % MAA almost corresponds to the minimum content producing noncrystallinity for E-MAA.

Before discussing the endothermic peak at 322 K of E-0.133MAA, let us mention the results of E-0.133MAA-0.6Na first. E-0.133MAA-0.6Na shows a faint hump at around 332 K in the $V(T)-T$ curve (in (b)), and in the DSC heating curve (in (d)), correspondingly, an endothermic peak is seen at 337 K whose onset temperature is 330 K. The peak temperature and the enthalpy change varied with aging time at room temperature. Figure 4 shows the DSC thermograms of E-0.133MAA-0.6Na as a function of aging time at room temperature. The peak observed on the first heating (1H) was absent on the subsequent cooling (1C) and heating (2H) runs immediately after the 1H run. When the sample was stored at room temperature for 1 day (in (a)), a very faint peak reappeared around 330 K, and as the aging time at room temperature increases (from (b) to (e)), its

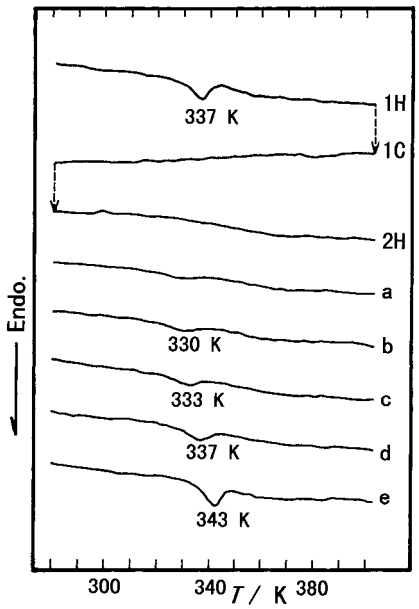

Figure 4. DSC curves for E-0.133MAA-0.6Na: 1H, first heating; 1C, first cooling; 2H, second heating immediately after the 1C scan; 2H scans after aging at room temperature for (a) 1, (b) 5, (c) 9, (d) 25, and (e) 46 days.

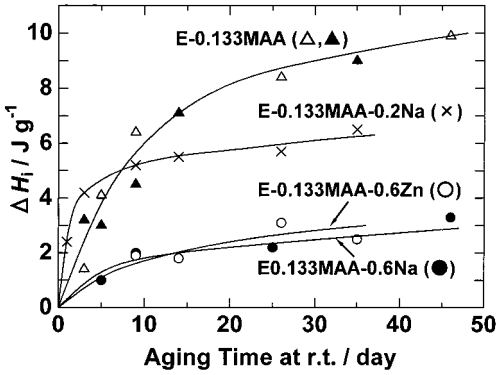

Figure 5. Plots of enthalpy change at T_i (ΔH_i) versus aging time at room temperature for various E-0.133MAA ionomers: E-0.133MAA (△, ▲), E-0.133MAA-0.2Na (×), E-0.133MAA-0.6Na (●), and E-0.133MAA-0.6Zn (○), where solid curves are only guides for the eye.

location shifted to higher temperatures and the enthalpy change became larger. After being aged for about 30 days (in (d) or (e)), the peak was almost located at the original temperature, and the enthalpy change of the peak was also restored to the original value. These observations are identical with a relaxational phenomenon during room-temperature aging of partly crystalline E-MAA ionomers, where the 330 K peak is assigned to an order−disorder transition associated with ionic aggregate regions, and the transition and its transition temperature are both labeled T_i. Therefore, the 330 K peak of E-0.133MAA-0.6Na is also assigned to T_i. Figure 5 shows plots of the enthalpy change at T_i (ΔH_i) versus the aging time at room temperature for all E-0.133MAA polymers. This result indicates that the T_i peak and its relaxational phenomenon are common in all E-0.133MAA polymers including the acid form. Thus, an important conclusion is derived that the T_i peak is observed independent of polyethylene crystallinity.

As briefly mentioned in the Introduction, the order−disorder transition model of ionic aggregate regions depicts the following picture. As proposed by Yarusso and Cooper,[51,52] the ionic aggregate region contains ionic

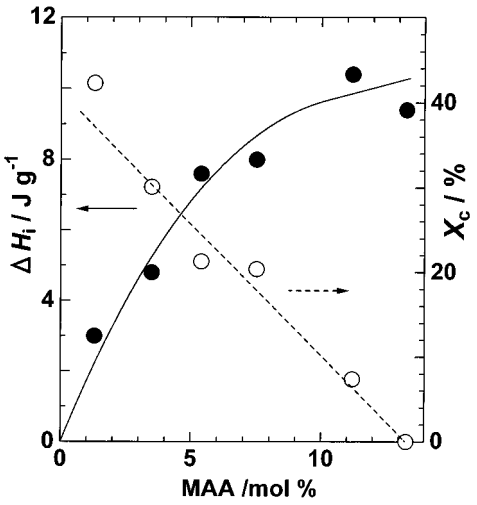

Figure 6. Plots of the enthalpy change at T_i (ΔH_i) and the degree of polyethylene crystallinity (X_c) versus the content of MAA for E-MAA acids.

side groups and a small portion of backbones drawn by the side groups; the ionic side groups primarily build a core of the aggregate region, and most of the backbones are probably present in the peripheral region of the ionic core.[31,32] In our original model,[25−27] the word "ionic cluster" was used, but this does not necessarily mean Eisenberg's ionic cluster. Inside the ionic core, which seems to correspond to Eisenberg's multiplet, we postulate that the ionic groups are arranged to have a local structural order as pointed out by Yarusso et al.[44] The local structural order is partly lost above T_i, and the state of ionic aggregate regions is turned to the *disordered* state. Since the movements of ionic groups and backbones in the aggregate region are constrained by each other, the reorganization from the disordered state toward the *ordered* one with an optimal arrangement including the arrangement of short segments of backbones would require some time, which we considered causes the above relaxational process.

Back to Figure 3, we assign an endothermic peak at 322 K (the onset temperature: 319 K) of E-0.133MAA to also T_i. The enthalpy change of this peak (∼9 J/g) was larger than the corresponding value (∼3 J/g) of E-0.133MAA-0.6Na. This seems to contradict the assignment that the peak is associated with some change of the ionic aggregate region because E-0.133MAA has no ionic groups. In sulfonated polystyrene ionomers, it is known that the acid polymers show an ionic peak due to the aggregation of acid groups in the SAXS region.[51] Although not evident from our SAXS results, it is possible that COOH groups of E-0.133MAA form some aggregation more than the dimerization, and this aggregation would undergo a transformation at T_i.[27] Figure 6 plots the values of ΔH_i and polyethylene crystallinity X_c of E-MAA acids versus the MAA content, where the samples were aged at 293 K for 30 days. As already mentioned, the X_c value almost linearly decreases, while the ΔH_i value monotonically increases with increasing MAA content. Furthermore, our dielectric results, described in the next, reveal that the fraction of dissociated COOH groups of E-0.054MAA at 330 K above T_i is ∼0.08 while that of E-0.133MAA is ∼0.115, 40% larger. This magnitude of increase is roughly equal to the increase (∼25%) of ΔH_i value. These results, although they are not a direct evidence of, are consistent with our assignment of the T_i peak of

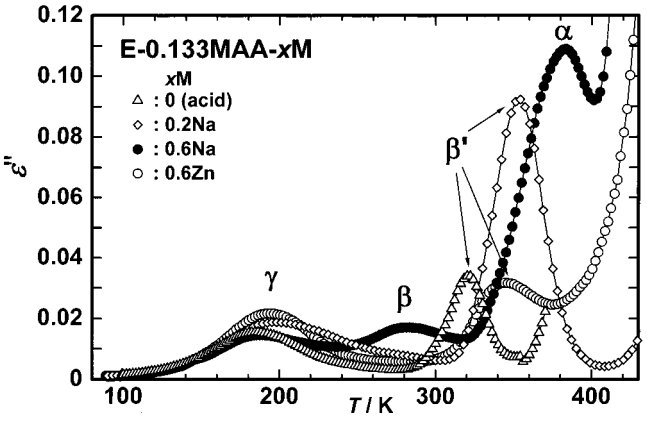

Figure 7. Temperature dependence of dielectric loss (ϵ'') at 1 kHz for E-0.133MAA (△), E-0.133MAA-0.2Na (◇), E-0.133MAA-0.6Na (●), and E-0.133MAA-0.6Zn (○). Four types of relaxations labeled γ, β, β', α are seen in going from the low-temperature side.

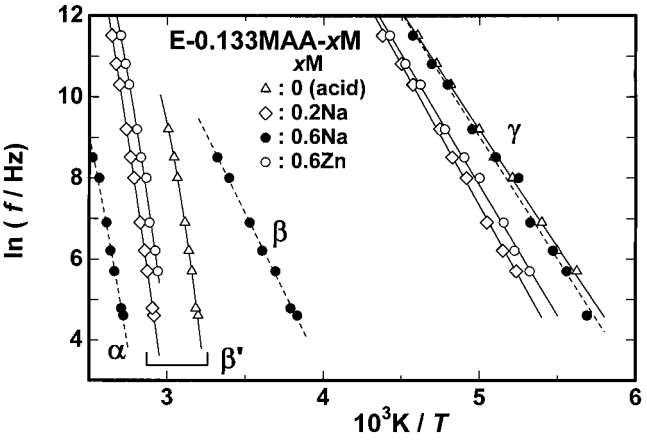

Figure 8. Arrhenius plots of relaxation frequency (f) versus relaxation temperature (T_{max}) for four relaxations (α, β, β', γ): E-0.133MAA (△), E-0.133MAA-0.2Na (◇), E-0.133MAA-0.6Na (●), and E-0.133MAA-0.6Zn (○). Solid and broken curves are guides for the eye.

acid E-MAA. For an extreme case, poly(acrylic acid), various types of hydrogen-bonded forms of COOH groups have been observed by IR, Raman, and near-IR spectroscopic measurements, and the presence of oligomeric forms is revealed in addition to the presence of the monomer and cyclic dimer forms.[53] The bandwidth (28 cm^{-1}) of the IR ν(C═O) band of E-0.133MAA is larger than that of E-0.054MAA (15 cm^{-1}), which suggests such possibility. To confirm this further, the temperature variation measurement of the spectra is necessary and currently progressing.

Dielectric Relaxation. Figure 7 shows the temperature dependence of dielectric loss (ϵ'') at 1 kHz for E-0.133MAA, E-0.133MAA-0.2Na, E-0.133MAA-0.6Na, and E-0.133MAA-0.6Zn. The Arrhenius plots of the relaxation frequency (f) versus temperature (T_{max}) for each relaxation are shown in Figure 8, from which the activation enthalpies (ΔH) at 1 kHz were obtained and are listed in Table 3. The observed relaxations were assigned on the basis of the temperature observed and ΔH value of each relaxation and with the aid of the previous publications.[22,23,28,29,54] In Figure 7, E-0.133MAA has two relaxations near 190 and 320 K, labeled γ and β'. The γ relaxation is ascribed to a local molecular motion of the short segments in the amorphous region. The β' relaxation is assigned to a micro-Brownian motion of long chain segments in the amorphous region, where COOH dimers primarily act as a cross-link and restrict that motion below T_g (T_g = 286 K by DSC) of the backbone. This behavior is essentially identical with that of E-0.054MAA whose MAA content is much lower. Neutralization of E-0.133MAA with sodium by 20% shifted β' relaxation to a temperature about 30 K higher, apparently due to the formation of ionic aggregates acting as cross-links. The same situation is seen for E-0.133MAA-0.6Zn, where the neutralization with Zn(II) is 60%. On the contrary, E-0.133MAA-0.6Na exhibited three relaxations labeled γ, β, α in going from low-temperature side, and the α relaxation temperature at 1 kHz is 383 K, much higher than the β' relaxation temperatures of other three E-0.133MAA polymers. Among three relaxations, the assignment of the γ relaxation is common to the γ of other E-0.133MAA polymers, but the β and α relaxations are generally ascribed respectively to a micro-Brownian motion of long chain segments containing Na salt groups isolated and dispersed in the amorphous region and to a micro-Brownian motion of long chain segments containing Na salt groups that are incorporated into the ionic aggregate region.

The replacement of β' relaxation by α and β relaxations is regarded as an indication of an enhanced microphase separation of ionic aggregate region from the polymer matrix, that is, the formation of a phase that has its own T_g. Such a phase was named an *ionic cluster* by Eisenberg and co-workers.[15] Along with this interpretation, the above dielectric studies derive a conclusion that E-0.133MAA-0.6Na has two T_g's, one from the ionic cluster and the other from the matrix, and the matrix becomes very similar to a branched polyethylene because most ionic groups are excluded from the matrix. On the other hand, E-0.133MAA-0.2Na and -0.6Zn have only one T_g, indicating that their ionic aggregates are almost isolated and dispersed in the matrix. This conclusion is in excellent agreement with the $p(r)$ function results from SAXS (see the section X-ray Scattering).

As easily expected, the phase separation behavior of E-MAA ionomers is dependent on the cation type and the degree of neutralization. Our previous dielectric and mechanical studies of E-0.054MAA ionomers[28,29,33] revealed that the ionic cluster phase is formed above ~30% neutralization in the Na salt whereas in the Zn(II) salt above 80% neutralization. Therefore, the present dielectric studies revealed an interesting fact that the phase separation of E-MAA ionomers is apparently governed by the degree of neutralization, although the ion content of E-0.133MAA ionomers is about 2.5 times higher than that of E-0.054MAA ionomers. The reason may be explained in terms of coordination chemistry of neutralizing cations.[12,33] The optimal number of oxygen atoms around Na^+ is 6, as seen in $NaH(CH_3COO)_2$, and the formation of the hexacoordination $(COO^-)Na^+(COOH)_2$ would be completed at 33% neutralization of the Na salt E-MAA ionomers. In the Zn(II) salt of E-0.133MAA, Zn(II) cations take a hexacoordination rather than tetracoordination structure, as mentioned in the section IR Spectra, and the formation of $(COO^-)_2Zn(II)(COOH)$ would be completed at 67% neutralization. In other words, below 33% neutralization for the Na salt and below 67% for the Zn salt, a considerable amount of unneutralized COOH dimers is present, restricting the mobility of long chain segments

Table 3. Dielectric Parameters of E-0.133MAA Ionomers[a]

	α		β′		β		γ	
sample	T_{max}, K	ΔH, kJ/mol	T_{max}, K	ΔH, kJ/mol	T_{max}, K	ΔH, kJ/mol	T_{max}, K	ΔH, kJ/mol
E-0.133MAA			321	208			185	47
E-0.133MAA-0.2Na			354	215			198	56
E-0.133MAA-0.6Na	383	169			284	62	188	49
E-0.133MAA-0.6Zn			347	216			194	52

[a] Assignments of α, β′, β, and γ relaxations are described in the text; T_{max} and ΔH, relaxation temperature and activation enthalpy at 1 kHz, respectively.

in the amorphous phase, where the β′ relaxation is activated. Therefore, the coordination chemistry predicts that the degrees of neutralization causing the phase separation are different between the two salts of E-MAA ionomers.

Quantitative Analysis of the Microphase Structure of E-0.133MAA Ionomers. When polar solutes with an effective dipole moment (μ) are dissolved in a nonpolar solvent and the dipoles are not so strongly correlated with each other, the number density (N) of the dipoles contributing to dielectric relaxations is obtained by using the Onsager equation:[55]

$$N\mu^2 = \frac{3k_BT}{4\pi}\left(\frac{2\epsilon_0 + \epsilon_\infty}{3\epsilon_0}\right)\left(\frac{3}{2+\epsilon_\infty}\right)^2(\epsilon_0 - \epsilon_\infty) \qquad (1)$$

where ϵ_0 and ϵ_∞ are the static and high-frequency limiting dielectric constants at a temperature T, respectively, and k_B is Boltzmann's constant. The values of ϵ_0 and ϵ_∞ are usually obtained from the Cole−Cole plots[56] or else estimated by using the following relations:

$$\epsilon_0 - \epsilon_\infty = \frac{2}{\pi R\left\langle\frac{1}{\Delta H}\right\rangle^{-1}}\int_0^\infty \epsilon'' \, \mathrm{d}\left(\frac{1}{T}\right) \qquad (2)$$

$$\epsilon_0 + \epsilon_\infty = 2\epsilon' \qquad (3)$$

where ΔH is the activation energy for the loss process, and $\langle\ \rangle$ denotes an average value over the measured frequency range; R is the gas constant. Equation 2 was derived by Read and Williams,[57] and eq 3 is based on an assumption that at a given temperature the Cole−Cole plot is symmetric with respect to the ϵ' value at a frequency at which the corresponding ϵ'' value shows a maximum. We regarded E-MAA ionomers simply as a solution in which polar side groups are dissolved in nonpolar polyethylene solvent. Although the polar groups might be correlated, we postulated that eq 1 is applicable for α relaxation above T_i and β/β′ relaxation above T_g in the present ionomers.

Figure 9 plots the value of $N\mu^2$ against T for E-0.133MAA ionomers including the acid form. Neglecting the contribution from the polyethylene matrix (which is reasonable for our approximate evaluation), the obtained value of $N\mu^2$ is resolved into three components: $N\mu^2 = \sum(N\mu^2)_i$, where $i = 0$, 1, and 2 are denoted as COOH, COONa/COO(Zn(II))$_{1/2}$ that contributes to the β/β′ relaxation, and COONa/COO(Zn(II))$_{1/2}$ contributing to the α relaxation, respectively. The third component (i.e., $i = 2$) is associated with the MAA side groups that are incorporated into the ionic cluster phase. E-0.133MAA has an $i = 0$ component only, and E-0.133MAA-0.2Na and E-0.133MAA-0.6Zn have $i = 0$ and 1 components, whereas E-0.133MAA-0.6Na has all three components.

As might be expected, the primary form of COOH in E-0.133MAA is hydrogen-bonded cyclic dimer, which, however, does not contribute to the $N\mu^2$ value because the dipole moment is zero. Although there is a possibility for the presence of other hydrogen-bonded forms with a nonzero dipole moment, for simplicity, we consider the contribution only from the simple monomeric form of COOH groups, whose dipole moment is $\mu = 1.7$ D (1 D $= 1.2 \times 10^{-18}$ esu cm).[58] Since the total number of COOH groups (both dimerized and dissociated) can be calculated by using the specific volume data (see Table 2) and the MAA content, we can evaluate the degree of dissociation, α, which is defined as the fraction of monomeric COOH groups to the total. The result is α = 0.115 for E-0.133MAA at 330 K, and by the same method, α = 0.08 was obtained for E-0.054MAA at 330 K. Note that the α value of E-0.133MAA at 330 K is about 40% larger than the corresponding value of E-0.054MAA. The large value of α of E-0.133MAA suggests that a relatively large value of ΔH_i of the sample mentioned in the section DSC and Dilatometry is related to the dissociation of COOH. Of course, α and thus $(N\mu^2)_0$ are temperature-dependent. Although, in a limited temperature range, μ was found to be well reproduced numerically by an equation of $\mu = AT + B$, where A and B are temperature-independent constants. Unfortunately, an abrupt increase of ϵ' above ∼330 K made the precise determination difficult, and we were unable to confirm whether some change occurs or not on $N\mu^2$ above T_i.

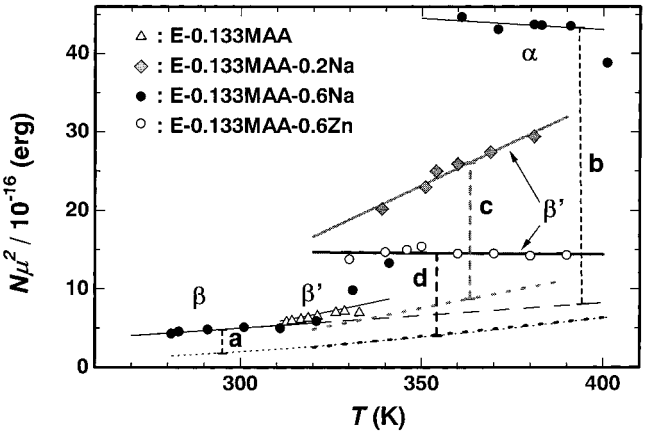

Figure 9. Plots the total value of $N\mu^2$ against T for E-0.133MAA (△), E-0.133MAA-0.2Na (◇), E-0.133MAA-0.6Na (●), and E-0.133MAA-0.6Zn (○). μ and N are the effective dipole moment and the number density, respectively. Dotted curves and notations *a*, *b*, *c*, and *d* are described in the text.

For E-0.133MAA-0.6Na (filled circle), the value of $N\mu^2$ is resolved into three components, the way of which is presented in Figure 9. The thin dotted curve represents the $(N\mu^2)_0$ component, which is given by the $N\mu^2$ value of E-0.133MAA multiplied by 0.4. Here, it was assumed that the state of COOH groups in E-0.133MAA-0.6Na is identical to that in E-0.133MAA and the temperature behavior of $\mu = AT + B$ is valid in the whole temperature range. Thus, the $(N\mu^2)_1$ component is given as the

difference denoted as *a*, in the temperature range below 320 K. Finally, the difference between the extrapolated line (thin broken line) and the observed value above 360 K, denoted as b, corresponds to the $(N\mu^2)_2$ component. For E-0.133MAA-0.2Na (rectangle) and E-0.133MAA-0.6Zn (unfilled circle), the differences denoted as *c* and *d* correspond to the $(N\mu^2)_1$ components of these ionomers, respectively.

The value $\mu = 6.5$ D was used for COONa,[59] and in the case of $COO(Zn(II))_{1/2}$, $\mu = 0.7$ D was chosen from the value of a model compound (bis(acetylacetone) complex of Zn(II)).[58] Using these values, the following quantitative information on the number of COONa groups associated with $\alpha/\beta/\beta'$ relaxation was obtained:

(1) In E-0.133MAA-0.2Na, the fraction of COONa activated by β' relaxation is 7.2−10% of the total (depending on *T*), and the corresponding value of E-0.133MAA-0.6Zn is almost 100%.

(2) In E-0.133MAA-0.6Na, the fraction of COONa groups activated by α relaxation is 5.2−6.4%, and that by β relaxation is ∼0.5%, of the total. As mentioned above, COONa groups activated by the α relaxation are incorporated into the ionic cluster, and the groups activated by the β relaxation are in the remaining unclustered region. If the groups associated with the β relaxation are also activated by the α relaxation and the fractions of COONa groups activated in both unclustered and clustered regions are the same, we can estimate that in E-0133MAA-0.6Na only about 10% (∼(0.5/(6−0.5)) of COONa groups are in the unclustered region and most (∼90%) of the COONa groups are in the cluster region.

The above evaluation is based on many assumptions and simplifications. Nevertheless, the obtained conclusions are quite reasonable. That is, point 1 for E-0.133MAA-0.6Zn and point 2 are well consistent with the SAXS conclusion that the fraction of the side groups incorporated into aggregates (β) is 0.09 for E-0.133MAA-0.6Zn and $\beta = 1.0$ for E-0.133MAA-0.6Na (see the section X-ray Scattering and Table 1).

Comparison with Partly Crystalline E-MAA Ionomers. By the same evaluation, a preliminary study for partly crystalline E-0.054MAA-0.6Na with an X_c value of 13% revealed that the fraction of COONa groups in the cluster region is about 80%, and for E-0112MAA-0.6Na with an X_c value of 7%, the corresponding fraction was about 85%.[60] From the SAXS studies, on the other hand, the size parameters of ionic aggregates were estimated at $R_1 = 6.3$ Å and $R_{ca} = 8.7$ Å for E-0.054MAA-0.6Na and $R_1 = 5.9$ Å and $R_{ca} = 7.9$ Å for E-0.112MAA-0.6Na, although these estimations may contain slightly larger errors because of their crystallinity. Hence, by increasing the MAA content from 5.4 mol %, the size of ionic aggregate slightly decreases but the fraction of COONa groups contributing to the cluster increases. These results also indicate the continuity of the microphase structure from partly crystalline to noncrystalline E-MAA ionomers.

In the next three sections, we will discuss the second objectives of this study: the factors that would be critical for the DSC T_i peak.

***T_i* and Water Absorption.** As mentioned in the Introduction, Cooper and co-workers[20] pointed out that water absorption during aging was the main origin of the change of DSC curve with time as seen in Figure 4. Despite the careful storage using a vacuum desiccator, our samples contained a small amount of water, as mentioned in the Experimental Section. However, our previous work[31,32] reveals that, in the case of partly crystalline E-0.054MAA ionomers, water absorption certainly affects the T_i peak but rather reduces it. To confirm the possibility pointed out by Cooper et al. for the present E-0.133MAA system, two types of experiments were conducted.

In the first experiment, the samples that had been already stored at room temperature for more than 1 month were kept under a different relative humidity (RH) atmosphere for an additional 14−15 days, and then the DSC scans were carried out. The results for E-0.133MAA-0.6Na showed that for the initial "dry" sample containing 0.7 wt % of water, the T_i and ΔH_i were 349 K and 4.6 J/g, respectively, which changed to 333 K and 2.5 J/g, respectively, by storing under 32% RH atmosphere to increase the absorbed water to 1.5 wt % and to 322 K and 3.0 J/g, respectively, when the sample was stored under 44% RH atmosphere and absorbed 2.5 wt % of water; water absorption shifted T_i to lower temperatures and decreased ΔH_i, and a similar trend was observed for all other E-0.133MAA ionomers.

In the second experiment, the sample was first dried in a vacuum at 423 K for 1 h and heated again to 433 K and cooled to room temperature at a rate of 10 K/min by using a DSC instrument. This sample was then stored at room temperature in a vacuum desiccator that was evacuated by a rotary pump every 12 h. After 8 days storage, E-0.133MAA-0.6Na, for example, showed an endothermic peak with $\Delta H_i = 1.0$ J/g at 335 K on the first heating run (10 K/min), where the weight change during the storage was found less than 0.1 wt %. These two results clearly reveal that E-0.133MAA ionomers without water absorption also show the DSC T_i peak and that water absorption certainly affects the peak but never enhances it.

***T_i* and Polyethylene Crystallites.** Cooper's first assignment[9] related the T_i anomaly to the formation of so-called imperfect crystallites of polyethylene short segments by room-temperature aging and its melting on heating. This possibility was examined by our earlier publications using dc conductivity measurements.[34,35] This technique can be a sensitive probe for internal changes in polymers, because internal changes strongly affect the state of the ionic conduction paths (usually formed in the amorphous regions). For partly crystalline E-0.054MAA ionomers,[34] it was found that the conductivity (σ) versus the reciprocal temperature ($1/T$) curve shows a small hump at a temperature very close to the DSC T_i and a bend at the melting point (T_m) of polyethylene crystallites and that when ionic aggregation causes an extensive microphase separation, i.e, ionic cluster, the former hump changes into a peak; the hysteresis of the σ peak observed is reminiscent of the behavior of the DSC T_i peak as shown in Figure 4. Clearly, the ionic groups in E-MAA ionomers are responsible for these σ anomalies.

When annealing this ionomer at 343 K below T_m for 5 min, the DSC curve on the subsequent heating showed another endothermic peak at a temperature ∼5 K higher than the annealing temperature, in addition to the T_i and T_m peaks. Clearly, this additional peak originates from the melting of imperfect polyethylene crystallites formed by the annealing. The annealing peak, however, did not cause any anomaly such as a bend or a peak on the $\sigma - 1/T$ curve. This result excludes the possibility that the DSC T_i peak is merely due to

the melting of imperfect crystallites formed by room-temperature aging.

As shown in Figures 4 and 5, an important conclusion of the present studies is that even noncrystalline E-0.133MAA ionomers exhibit a DSC T_i peak. As presented by Figure 7 of ref 35, the $\sigma-1/T$ curves of E-0.133MAA-0.6Na and -0.6Zn exhibit an evident peak at a temperature corresponding to DSC T_i, above which no other anomalies were observed, consistent with our interpretation mentioned here.

Glass Transition Nature of the T_i "Transition". As described in the section Dielectric Relaxation, the α relaxation is observed above T_i, as a result of softening of ionic aggregate region which enables a micro-Brownian molecular motion of long segments linked to the ionic aggregates. In *unclustered* ionomers, the β' relaxation is observed at a temperature very close to T_i and assigned to a micro-Brownian molecular motion of long segments to which ionic groups are attached. These suggest that T_i is a temperature at which ionic aggregates lose their ability to restrain the mobility of chain segments attached to them; that is, the T_i anomaly has a glass transition nature.[34,37]

In connection with this, Eisenberg et al.[16] argued that ion hopping proceeds at an appreciable rate at temperatures near the glass transition temperature of ionic aggregate region, where an inflection point of log(storage modulus) versus temperature curve is regarded as the onset temperature of ion hopping, labeled the same code T_i as used for an order−disorder transition temperature of ionic aggregate region. The ion-hopping temperature T_i is very similar to our assignment of T_i in E-MAA ionomers, in that both T_i temperatures are due to changes in the ionic aggregate regions; above these temperatures, the ionic aggregate region partly loses its functionality and changes from a rigid cross-link to a soft one.[34,37]

A difference between Eisenberg's model and ours is that the former did not consider the existence of any orderness inside the ionic aggregate core, while our model postulates some organization of ionic side groups because the dipole moments are arranged in an energetically favorable way, although subject to some constraint from the backbone. An important point is that the backbone of the E-MAA ionomer system is primarily polyethylene, with a small portion of MAA units, which is much more flexible than *atactic* polystyrene of the system on which Eisenberg's model is based; in the E-MAA ionomer system, an ordered packing of ionic groups inside the aggregate can be realized. In fact, in this study, it was revealed that the coordination structure around Zn(II) in the Zn(II) salts of E-MAA ionomers depends on the MAA content, which indicates that the coordination structure is strongly governed by the flexibility of the backbone. In our previous report on E-0.054MAA-0.6Co, it was shown that the hexacoordination structure around Co(II) is transformed into the tetracoordination around T_i,[36] which is an evidence supporting that the ionic aggregate changes at T_i.

The DSC T_i peak is observed even in the acid precursor as well as unclustered E-MAA ionomers. Since E-MAA acids are generally considered to have no ionic aggregates, this was regarded as a failure of our model and inclined people to consider a contribution of imperfect polyethylene crystallites to the DSC T_i peak, but the interpretation does not necessarily explain all the experimental results, as have been seen in the preceding section. We believe the presence of some aggregation of acid groups is responsible for that (see the section DSC and Dilatometry).

In connection with the glass transition nature of the DSC T_i peak, one would point out a possibility of enthalpy relaxation of the glassy state during room-temperature aging.[61] In sulfonated *atactic* polystyrene ionomers, Weiss[62] reported that the aging at room temperature below T_g (=370−390 K) of *atactic* polystyrene changes the DSC curve with a simple step at the T_g into a step followed by an endothermic peak in the high-temperature side and that this tendency is more evident at higher ion content. These results were interpreted as an enthalpy relaxation of the glassy polystyrene matrix. If T_i were regarded as the glass transition temperature of ionic aggregate region despite clustered or not, it could be considered that the DSC T_i peak results from enthalpy relaxation of *glassy* ionic aggregate region. However, increasing the MAA content from 5.4 mol % conversely reduces the magnitude of the DSC T_i peak, which contradicts the possibility. Of course, a more systematic investigation on the MAA dependence is apparently necessary and now in progress.

At this stage, we cannot but consider that the T_i anomaly is a complex phenomenon and more than one process takes place at and around the DSC T_i. However, it is very certain that the state of ionic aggregate region is changed at T_i.

Concluding Remarks

The present studies have revealed some quantitative features of microphase structure of noncrystalline E-0.133MAA ionomers by using IR, DSC, X-ray scattering, and dielectric relaxation measurements. The structural features obtained are the following: In 60% neutralized Na salt (E-0.133MAA-0.6Na), the ionic aggregate has an ionic core with a radius of ∼6 Å and incorporates almost 100% of MAA side groups including unneutralized COOH in the sample into it; ∼9 MAA side groups per aggregate. The ionic aggregate of this ionomer forms a microphase-separated ionic cluster, in which the most (∼90%) of COONa groups are present. On the other hand, in both 60% neutralized Zn salt (E-0.133MAA-0.6Zn) and 20% neutralized Na salt (E-0.133MAA-0.2Na), the core size is 4−5 Å, smaller than that of E-0.133MAA-0.6Na. The aggregate contains 3−6 MAA side groups and is almost isolated and dispersed in the matrix. The present studies have demonstrated that the coordination chemistry of neutralizing cations plays an important role in ionic aggregation and the formation of microphase-separated ionic cluster in E-MAA ionomers.

Another finding is that these *noncrystalline* E-0.133MAA ionomers exhibit a DSC T_i peak accompanied by a characteristic relaxation during room-temperature aging, similarly to partly crystalline E-MAA ionomers. This finding strongly supports that the DSC T_i peak is associated with changes of the state of ionic aggregate region.

Acknowledgment. We thank Mr. Yoshikazu Kutsuwa of Technical Center, Du Pont-Mitsui Polychemicals Co., Ltd., Chiba, Japan, for his encouragement and very helpful discussions. We also thank Mr. Tomomi Ikeno, Mr. Shunichi Osada, Mr. Satoshi Itoh, and Mr. Yoshiaki Satoh of Gifu University for their helps in SAXS and DSC measurements. This work was partly

supported by Grant-in-Aid for Scientific Research (No. 07650797) from the Ministry of Education, Science, and Culture, Japan. The SAXS experiments were performed under the approval of the Photon Factory Program Advisory Committee (proposals 91-100, 92G309, and 94-G125), and we are grateful to Prof. Katsumi Kobayashi of the National Laboratory for High Energy Physics for his guidance and kind help.

References and Notes

(1) Rees, R. W.; Vaughan, D. J. *Polym. Prepr.* (*Am. Chem. Soc., Div. Polym. Chem.*) **1965**, *6*, 287.
(2) Rees, R. W.; Vaughan, D. J. *Polym. Prepr.* (*Am. Chem. Soc., Div. Polym. Chem.*) **1965**, *6*, 296.
(3) *Ionic Polymers*; Holliday, L., Ed.; Applied Science: London, 1975.
(4) Eisenberg, A.; King, M. *Ion-Containing Polymers, Physical Properties and Structure, Polymer Physics*; Academic Press: New York, 1977; Vol. 2.
(5) *Structure and Properties of Ionomers*; Pineri, M., Eisenberg, A., Eds.; NATO ASI Series C, Mathematical and Physical Sciences; D. Reidel: Dordrecht, The Netherlands, 1987; Vol. 198.
(6) *Ionomers: Characterization, Theory, and Applications*; Schlick, S., Ed.; CRC Press: Boca Raton, FL, 1996.
(7) *Ionomers: Synthesis, Structure, Properties and Applications*; Tant, M. R., Mauritz, K. A., Wilkes, G. L., Eds.; Blackie Academic and Professional: London, 1997.
(8) Marx, C. L.; Cooper, S. L. *Makromol. Chem.* **1973**, *168*, 339.
(9) Marx, C. L.; Cooper, S. L. *J. Macromol. Sci., Phys.* **1974**, *B9*, 19.
(10) MacKnight, W. J.; Taggart, W. P.; Mckenna, L. *J. Polym. Sci., Symp.* **1974**, *46*, 83.
(11) Tsujita, Y.; Shibayama, K.; Takizawa, A.; Kinoshita, T.; Uematsu, I. *J. Appl. Polym. Sci.* **1987**, *33*, 1307.
(12) Hirasawa, E.; Yamamoto, Y.; Tadano, K.; Yano, S. *J. Appl. Polym. Sci.* **1991**, *42*, 351.
(13) Bruce Orler, E.; Moore, R. B. *Macromolecules* **1994**, *27*, 4774.
(14) Quiram, D. J.; Register, R. A.; Ryan, A. J. *Macromolecules* **1998**, *31*, 1432.
(15) Eisenberg, A.; Hird, B.; Moore, R. B. *Macromolecules* **1990**, *23*, 4098.
(16) Kim, J.-S.; Eisenberg, A. In ref 6, p 7.
(17) Risen, W. J., Jr. In ref 6, p 281.
(18) Longworth, R.; Nagel, H. In ref 7, p 365.
(19) Longworth, R.; Vaughan, D. J. *Nature (London)* **1968**, *218*, 85.
(20) Goddard, R. J.; Grady, B. P.; Cooper, S. L. *Macromolecules* **1994**, *27*, 1710.
(21) MacKnight, W. J.; McKenna, L. W.; Read, B. E. *J. Appl. Phys.* **1967**, *38*, 4208.
(22) Read, B. E.; Carter, E. A.; Connor, T. M.; MacKnight, W. J. *Br. Polym. J.* **1969**, *1*, 123.
(23) Phillips, P. J.; MacKnight, W. J. *J. Polym. Sci., Part A-2* **1970**, *8*, 727.
(24) Kajiyama, T.; Oda, T.; Stein, R. S.; MacKnight, W. J. *Macromolecules* **1971**, *4*, 198.
(25) Tadano, K.; Hirasawa, E.; Yamamoto, Y.; Yamamoto, H.; Yano, S. *Jpn. J. Appl. Phys.* **1987**, *26*, L1440.
(26) Tadano, K.; Hirasawa, E.; Yamamoto, H.; Yano, S. *Macromolecules* **1989**, *22*, 226.
(27) Hirasawa, E.; Yamamoto, Y.; Tadano, K.; Yano, S. *Macromolecules* **1989**, *22*, 2776.
(28) Yano, S.; Yamamoto, H.; Tadano, K.; Yamamoto, Y.; Hirasawa, E. *Polymer* **1987**, *28*, 1965.
(29) Yano, S.; Nagao, N.; Hattori, M.; Hirasawa, E.; Tadano, K. *Macromolecules* **1992**, *25*, 368.
(30) Tsunashima, K.; Nishioji, H.; Hirasawa, E.; Yano, S. *Polymer* **1992**, *33*, 1809.
(31) Kutsumizu, S.; Nagao, N.; Tadano, K.; Tachino, H.; Hirasawa, E.; Yano, S. *Macromolecules* **1992**, *25*, 6829.
(32) Yano, S.; Tadano, K.; Nagao, N.; Kutsumizu, S.; Tachino, H.; Hirasawa, E. *Macromolecules* **1992**, *25*, 7168.
(33) Tachino, H.; Hara, H.; Hirasawa, E.; Kutsumizu, S.; Tadano, K.; Yano, S. *Macromolecules* **1993**, *26*, 752.
(34) Kutsumizu, S.; Hashimoto, Y.; Hara, H.; Tachino, H.; Hirasawa, E.; Yano, S. *Macromolecules* **1994**, *27*, 1781.
(35) Kutsumizu, S.; Hashimoto, Y.; Sakaida, Y.; Hara, H.; Tachino, H.; Hirasawa, E.; Yano, S. *Macromolecules* **1994**, *27*, 5457.
(36) Kutsumizu, S.; Kimura, H.; Mohri, F.; Hara, H.; Tachino, H.; Hirasawa, E.; Yano, S. *Macromolecules* **1996**, *29*, 4324.
(37) Kutsumizu, S.; Hara, H.; Tachino, H.; Shimabayashi, K.; Yano, S. *Macromolecules* **1999**, *32*, 6340.
(38) Lee, J. Y.; Painter, P. C.; Coleman, M. M. *Macromolecules* **1988**, *21*, 346.
(39) Ueki, T.; Hiragi, Y.; Kataoka, M.; Inoko, Y.; Amemiya, Y.; Izumi, Y.; Tagawa, H.; Muroga, Y. *Biophys. Chem.* **1985**, *23*, 115.
(40) Part 1 of this series: Kutsumizu, S.; Tagawa, H.; Muroga, Y.; Yano, S. *Macromolecules* **2000**, *33*, 3818.
(41) Koizumi, N.; Yano, S. *Bull. Inst. Chem. Res., Kyoto Univ.* **1969**, *47*, 320.
(42) For example: Han, K.; Williams, H. L. *J. Appl. Polym. Sci.* **1991**, *42*, 1845 and references therein.
(43) Coleman, M. M.; Lee, Y. T.; Painter, P. C. *Macromolecules* **1990**, *23*, 2339.
(44) Yarusso, D. J.; Ding, Y. S.; Pan, H. K.; Cooper, S. L. *J. Polym. Sci., Polym. Phys. Ed.* **1984**, *22*, 2073.
(45) Grady, B. P.; Floyd, J. A.; Genetti, W. B.; Vanhoorne, P.; Register, R. A. *Polymer* **1999**, *40*, 283.
(46) Ishioka, T. *Polym. J.* **1993**, *25*, 1147.
(47) Ishioka, T.; Shimizu, M.; Watanabe, I.; Harada, M.; Kawauchi, S. *Rep. Prog. Polym. Phys. Jpn.* **1997**, *40*, 447.
(48) Welty, A.; Ooi, S.; Grady, B. P. *Macromolecules* **1999**, *32*, 2989.
(49) Yano, S.; Nakamura, M.; Kutsumizu, S. *Chem. Commun.* **1999**, 1465.
(50) Longworth, R. In ref 3, p 69.
(51) Yarusso, D. J.; Cooper, S. L. *Macromolecules* **1983**, *16*, 1871.
(52) Yarusso, D. J.; Cooper, S. L. *Polymer* **1985**, *26*, 371.
(53) Dong, J.; Ozaki, Y.; Nakashima, K. *Macromolecules* **1997**, *30*, 1111 and references therein.
(54) McCrum, N. G.; Read, B. E.; Williams, G. *Anelastic and Dielectric Effects in Polymeric Solids*; John Wiley & Sons: New York, 1967.
(55) Onsager, L. *J. Am. Chem. Soc.* **1936**, *58*, 1486.
(56) Cole, K. S.; Cole, R. H. *J. Chem. Phys.* **1941**, *9*, 341.
(57) Read, B. E.; Williams, G. *Trans. Faraday Soc.* **1961**, *57*, 1979.
(58) McClellan, A. L. *Tables of Experimental Dipole Moments*; W. H. Freeman & Co.: San Francisco, 1963.
(59) Hodge, I. M.; Eisenberg, A. *Macromolecules* **1978**, *11*, 283.
(60) Tadano, K. Unpublished results.
(61) Petrie, S. E. B. *J. Polym. Sci., Part A-2* **1972**, *10*, 1255.
(62) Weiss, R. A. *J. Polym. Sci., Polym. Phys. Ed.* **1982**, *20*, 65.

MA0004256